Signal Processing 91 (2011) 1085–1092

Contents lists available at ScienceDirect

Signal Processing

journal homepage: www.elsevier.com/locate/sigpro

Image compressed sensing based on wavelet transform in contourlet domain ☆

Xue Bi [a,b,*], Xiang-dong Chen [a], Yu Zhang [c], Bin Liu [a]

[a] School of Information Science and Technology, Southwest Jiaotong University, Chengdu 610031, China
[b] Network Center, Xi Hua University, Chengdu 610039, China
[c] Drilling and Production Technology Research Institute, CNPC Chuanqing Drilling Engineering Company Limited, Guanghan 618300, China

ARTICLE INFO

Article history:
Received 23 November 2009
Received in revised form
26 August 2010
Accepted 12 October 2010
Available online 3 November 2010

Keywords:
Compressed sensing
Image reconstruction
Contourlet domain
Wavelet transform

ABSTRACT

Compressed sensing (CS) has been widely concerned and sparsity of a signal plays a crucial role in CS to exactly recover signals. Contourlet transform provides sparse representations for images, so an algorithm of CS reconstruction based on contourlet is considered. Meanwhile, taking into account the computation and the storage of large random measurement matrices in the CS framework, we are trying to introduce the wavelet transform into the contourlet domain to reduce the size of random measurement matrices. Several numerical experiments demonstrate that this idea is feasible. The proposed algorithm possesses the following advantages: reduced size of random measurement matrix and improved recovered performance.

1. Introduction

In conventional imaging systems, images are uniformly sampled first at a high rate, and then most of the sampling data are thrown away for the purpose of compression. A common question is why we acquire this rich data, just to use a little part of it and discard the most. Over the past few years, a new sampling theory called compressed sensing (CS) has emerged. It provides us a framework of acquiring and compressing signals simultaneously. The CS theory [1] states that if signals are sparse in some bases, then they will be recovered from a small number of random linear measurements via a tractable convex optimization program.

Therefore, the quality of reconstruction relies on the sparsity level of images. In fact, many images are sparse in some appropriate transform domain. Accordingly, images are recovered from fewer samples than the Nyquist rate in some transform domain, such as the work done by Tsaig and Donoho. In their researches [2], they proposed CS reconstruction based on the wavelet transform. However, some other emerging bases are able to provide sparser representations for signals than wavelet basis does. Then, in work [2], the authors put forward CS based on the curvelet transform, which offers two key features named directionality and anisotropy. Directionality referring to the transform provides a variety of directional representations for signals and anisotropy, means the transform uses various different long-shaped bases to capture contours. However, in work [3], the challenge for curvelets was stated as 'is there a spatial domain scheme for refinement which, at each generation doubles the spatial resolution as well as the angular resolution?' This challenge has led to the development of the discrete contourlet transform. The transform will still keep the key features of directionality and anisotropy, and thus it will provide images with sparse expansions. The sparsity plays a fundamental role in CS for

☆ This work is supported by the National Natural Science Foundation of China under the Grant Nos. 60871024 and 60572026. And it is also supported by Program for New Century Excellent Talents in University in Ministry of Education of China under the Grant No. A0160419950120.

* Corresponding author at: School of Information Science and Technology, Southwest Jiaotong University, Chengdu 610031, China. Tel.: +86 13880969326.

E-mail addresses: bisnowhappy@163.com (X. Bi), xdchen@home.swjtu.edu.cn (X.-d. Chen).

0165-1684/$ - see front matter © 2010 Elsevier B.V. All rights reserved.
doi:10.1016/j.sigpro.2010.10.006

Nomenclature

j	decomposed scale of the contourlet transform
j^*	decomposed scale of the wavelet transform
l_j	number of directional level in the contourlet domain
S_M	size of random measurement matrix.
$S_{\max}$	maximum size of the random measurement matrix.

efficiently reconstructing images. So we propose CS reconstruction in the contourlet domain, which is different from work [2].

From work [4], the input data of CS is the one-dimensional signal. When CS is applied into two-dimensional signals, we should transform them into one-dimensional signals. Accordingly, when CS framework is applied into two-dimensional contourlet subband, this subband needs converting into a long vector, which should be measured by a large random matrix generated soon after. And this large matrix will increase a great amount of computation and storage. So we propose that each sparse contourlet subband should be further transformed by wavelets, and then the gathered wavelet coefficients will be measured in the CS framework. Only the gathered coefficients rather than all coefficients are used in the CS framework, thus the size of the corresponding random matrix is reduced. Above all, in comparison with other CS reconstruction methods, the proposed method applies CS in contourlet domain, where the wavelet transform is introduced.

This paper is organized as follows: Section 2 firstly provides a review about CS framework and contourlet transform, and then wavelet transform into the contourlet domain is introduced. In Section 3, the author presents the algorithm of reconstructing images by CS based on wavelet transform in the contourlet domain. Section 4 shows the simulation results and is followed by conclusion in Section 5.

2. CS framework and contourlet transform

2.1. CS framework

CS is a very efficient and fast growing signal recovery framework. It aims at accurately reconstructing signals from a small number of linear non-adaptive measurements by using an optimization programming process. Given an N-dimensional real valued signal x, the CS model [1] is

$$\min||\alpha||_1 \quad \text{subject to} \quad y=\boldsymbol{\Phi}x=\boldsymbol{\Phi\Psi}\alpha \tag{1}$$

where y is an $n\times 1(n<\mathrm{N})$ sampling vector, Φ represents an $\mathrm{n}\times\mathrm{N}$ measurement matrix, Ψ is basis in which the signal has a sparse representation, α represents the transformed vector in basis Ψ, and $||\alpha||1$ namely the ℓ_1 norm of α denotes the sum of absolute value of nonzero components in α.

This reconstruction problem is equivalent to find sparse vector α through the convex optimization program. There are many optimal methods to solve this problem, for example basis pursuit (BP) [5], Bayesian CS (BCS) [6], StOMP (stagewise OMP) [7], and so on.

From the above model, CS contains two critical parts: random observation and sparsity.

Random observation, a surprising gift for signal processing, means we do not deliberately choose a matrix for observing signals. The work [1] stated 'we do not have to seek for a "special" subspace for projecting signals. Choosing a subspace in a completely random manner will work almost all of the time. The random observation refers to the measurement matrix Φ in Eq. (1). Until now, some references have proposed some observation matrices [8,9]. In this paper, we choose a uniformly random matrix Φ which samples signals independently and uniformly on the unit sphere.

Sparsity [9], we impose it on the coefficients of the transform domain, means signals mainly rely on the number of degrees of freedom that is much smaller than their original length. For example, most of the contourlet coefficients are small (near to zero) and the comparably few large coefficients retain the most important information of signals. Reorder these coefficients, they will decay rapidly satisfying a power-law decay [10,11]. From work [9], we know that if the transform coefficients of signals decay like a power-law, they will be recovered from CS.

The decay rate of coefficients in some bases is a criterion for judging their ability in sparse representation of signals. Different bases have different decay rates. A new generation of the wavelet-contourlet [10,11] discussed below provides a fast decay rate and sparse representations for images.

2.2. Contourlet transform and wavelet subspace

The contourlets [10] which possess the key features of directionality and anisotropy provide sparse expansions for images. Contourlet transform is realized by double filter bank named pyramid directional filter bank (PDFB). The first is the Laplacian pyramid (LP) filter [12] and the second is a directional filter bank (DFB) [13]. The PDFB decomposes an image into a lowpass subband and several bandpass subbands at multiscales.

Given the signal space $L^2(R^2)$ decomposed into multiscale and multidirectional subspaces by the contourlet transform.

$$L^2(R^2)=V_{j1}\oplus\left(\bigoplus_{j\le j1}\left(\bigoplus_{k=0}^{2^{l_j-1}}W_{j,k}^{(l_j)}\right)\right)$$

$$W_j=\bigoplus_{k=0}^{2^{l_{j-1}}}W_{j,k}^{(l_j)}$$

where V_{j1} and W_j are approximation subspace and detail subspaces, respectively; l_j is the number of directional level ($l_j\ge 2$), which can be different at different scales; W_j is decomposed into some directional subspaces $W_{j,k}^{l_j}$, which is shown in Fig. 1.

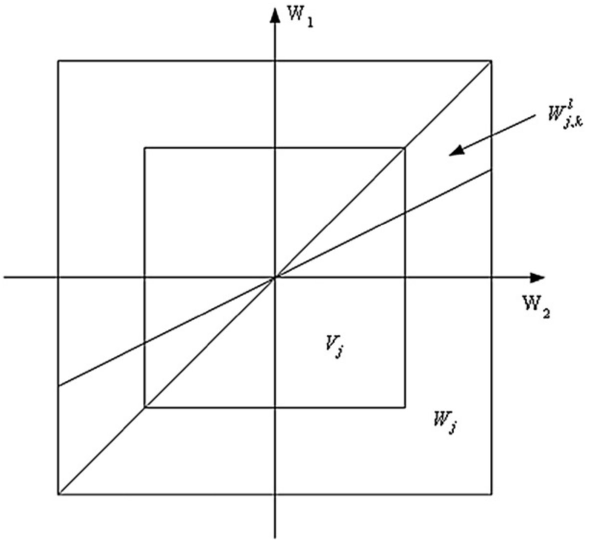

Fig. 1. Contourlet subspaces $W_{j,k}^{(l_j)}$, W_j and V_j illustrated on two-dimensional spectrum decomposition.

Fig. 2 shows an example of the contourlet coefficients of the ‘Sheep-Logan Phantom’ image. The image is decomposed into one pyramidal level, and it is then decomposed into eight directional subbands. Small coefficients are colored black, while large coefficients are colored white. We can see a small number of large coefficients. Thus the contourlet transform can effectively provide the sparse directional subbands for images.

The contourlets achieve the optimal nonlinear approximation behavior for piecewise smooth function, which is away from smooth contours. The decay rates of approximation error for images by different bases are listed in Table 1, where x is the original signal, M denotes the index of the M-largest coefficients in basis, and x_M is the M-term approximation of signal x. This table illustrates different bases with different decay rates.

From Section 2.1, we notice that a sparse expansion of image is of great importance for the CS reconstruction. Because of the optimal approximation rate, contourlet transform can be joined with CS, like the curvelet transform combined with CS [2].

Contourlet transform provides some sparse subbands that are required in CS; but computation and storage will increase when we generate large random matrices for each contourlet subband.

Let us have a size of $N\times N$ original image transformed by contourlet basis. For clear representation, the image is only decomposed into one pyramidal level and four directional subbands. From work [4], we should separately transform four two-dimensional subbands into a column vector, which means every subband is transformed into a long vector with the length of $(N^2/4)((N/2)\times(N/2))$. So a large random matrix should be generated to measure this long vector, which makes the computation and the storage very difficult.

For example, a $512\times 512(N=512)$ image is decomposed by contourlets. Then, each subband is converted into a long vector with the length of 65,536. In work [8], it pointed out that the number of sampling points of original signal is about four times of its sparsity level for reconstruction. For simplification, we uniformly assume the sparsity level of every transformed vector is 6554(65,536 $\times$ 0.1). Then, there are 2621(6554 $\times$ 4) sampling points and the size of random measurement matrix is (26,216 $\times$ 65,536). The image is decomposed into four subbands, and then there are four long vectors and four large random matrices need to be generated. Therefore, it is difficult and unavoidable to generate these matrices with large size when we directly apply CS reconstruction to sparse contourlet subbands without other transform stages.

Consequently, if the transformed coefficients are distributed concentratedly in some smaller subspaces, the size of the random matrix will be small and tractable. In this paper, we

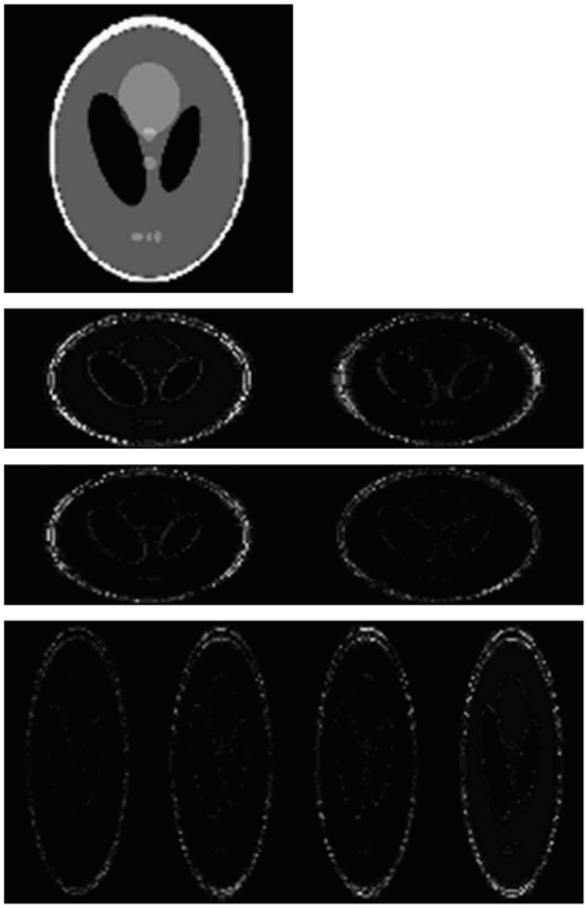

Fig. 2. Contourlet transform of the ‘Sheep-Logan Phantom’ image. The image is decomposed into one pyramidal level, and it is then decomposed into eight directional subbands.

Table 1
Decay rates of approximation error by different bases.

Type of basis	Decay rate (in an L_2-norm square$\|x-x_M\|_2^2$)
Contourlet basis [11]	$o(\log M)^3 M^{-2}$
Curvelet basis [14]	$o((\log M)^{1/2} M^{-2})$
Wavelet basis [11]	$o(M^{-1})$
Fourier basis [14]	$o(M^{-1/2})$

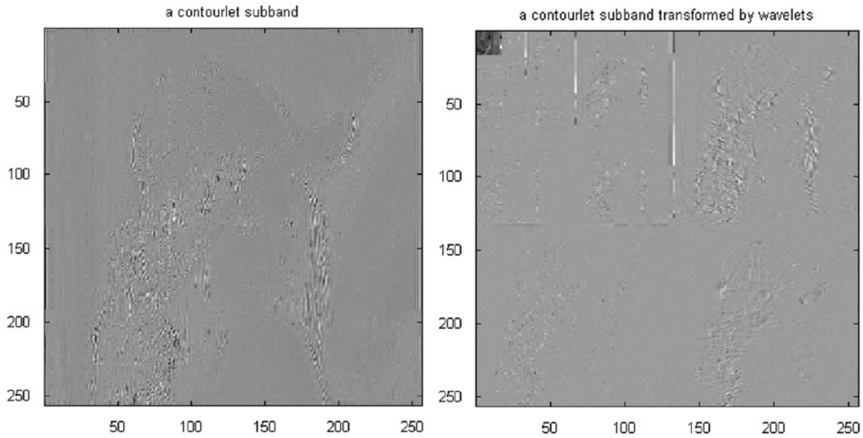

Fig. 3. Example of a 256×256 contourlet sub b and and its transformed result by wavelets.

propose that each contourlet subband is transformed by two-dimensional orthonormal wavelet bases, which make coefficients concentrated into some small subspaces of wavelet domain. Only the concentrated coefficients are used in the CS framework, so the size of random matrices is comparably small and they can be easily generated. Fig. 3 shows a contourlet subband and its transformed result by wavelet. The important information of the contourlet subband is concentrated into the wavelet domain, as shown in Fig. 3.

From the above descriptions, we show a 256×256 directional contourlet subband in Fig. 3(a) whose sparsity rate is also supposed as 0.1. Then the length of the transformed vector is 65536, and the size of the random observation matrix is ($26{,}216\times65{,}536$). In Fig. 3(b), we take the same contourlet subband and transform it by wavelets. The decomposition scales of wavelets are selected automatically and the corresponding subset of wavelet coefficients is also determined. Here, the coarse scale is 4 and the fine scales are 5 and 6. The size of concentrated part in the wavelet domain is less than (32×32) which is far less than (256×256). And the corresponding random matrix is much smaller than $26{,}126\times65{,}536$. Hence, when we introduce wavelet transform into the contourlet domain, both the length of corresponding transformed vector and the size of random matrix are decreased. This paper uses CS in these concentrated parts, which avoids generating large random matrices.

Therefore, we apply CS in the contourlet domain combined with wavelet transform to reconstruct images. We take the scheme of multiscale compressed sensing [2], using conventional linear sampling on coarse scale and applying CS to fine scales. Different fine scales are segregated and CS is applied separately to each scale. In this paper, the contourlet subbands are separately transformed by wavelets, and then multiscale compressed sensing is applied on each of them.

3. The proposed algorithm

The reconstruction algorithm consists of the following steps.

(1) Firstly, transform the input image x into several sparse directional contourlet subbands $x^{l_j}_{j,k}$. Pyramidal decomposed level j and the number of directional level l_j at each scale are selected automatically. When l_j is chosen, the range of direction k is $0\sim2^{l}_{j}-1$. j_0 denotes the coarse scale of contourlets, and the fine scale of contourlets is written as j_1. The coefficients of each contourlet subband are written as $C^{(l_j)}_{j,\,k}(j_0\le j\le j_1,\quad l_j\ge2,\quad 0\le k\le2^{l_j}-1)$[1]

(2) Orthonormal wavelet transform is applied to each $C^{(l_j)}_{j,\,k}$.

$$C^{(l_j)}_{j,\,k}=\sum_{j^*=j_{00}}^{j_{11}}\sum_{n}\alpha^{(l_j)}_{j^*,\,k,\,n}\psi_{j^*,\,n}+\sum_{n}\beta^{(l_j)}_{j_{00},\,k,\,n}\varphi_{j_{00},\,n}\tag{2}$$

where $C^{(l_j)}_{j,k}$ are expanded by ψ^*_j (wavelet function) and φ_j00 (scale function). The decomposed scale of wavelet j^* is selected from the coarse scale j_{00} to the fine scale j_{11}.

Adopt conventional linear sampling at coarse scales j_{00}, while apply CS scheme to fine scales (random sampling scales). Then, at each fine scale

$$y^{(l_j)}_{j^*,\,k}=\Phi_{j^*}\times\alpha^{(l_j)}_{j^*,\,k}\quad j^*=j_{00}+1,\ldots,j_{11}\tag{3}$$

where Φ_{j*} is an $n\times m$ uniform random measurement matrix and is separated at different wavelet scales of each subband, $m=4^{(j^*)}-4^{(j^*-1)}$. From the CS model, we know $n<$ m, so let n=cm, $0<c<1$.

(3) Solve the optimal problem (in this paper, we take BP and Bayesian).

$$\min\|\alpha^{(l_j)}_{j^*,\,k}\|_1\quad\text{subject to } y^{(l_j)}_{j^*,\,k}=\Phi_{j^*}\times\alpha^{(l_j)}_{j^*,\,k}\quad j^*=j_{00}+1,\ldots,j_{11}\tag{4}$$

$\hat{\alpha}^{(l_j)}_{j^*,\,k}$ is the solution, then we obtain $\hat{C}^{(l_j)}_{j,\,k}$ after the inverse wavelet transform

$$\hat{C}^{(l_j)}_{j,\,k}=\sum\nolimits_{j^*=j_{00}}^{j_{11}}\sum\nolimits_{n}\hat{\alpha}^{(l_j)}_{j^*,\,k,\,n}\psi_{j^*,\,n}+\sum\nolimits_{n}\beta^{(l_j)}_{j_{00},\,k,\,n}\varphi_{j_{00},\,n}\tag{5}$$

[1] An example of the contourlet subband $C^{(l_j)}_{j,\,k}$ is shown in Fig. 3(a).

(4) Even though the previous signal is noiseless, $\hat{C}_{j,k}^{(l_j)}$ have been mixed with some noise owing to random observations. So we take threshold [15] to denoise

$$th = \beta\sigma \quad \sigma = median|(d(\hat{C}_{j,k}^{(l_j)}))|/0.6745$$

where $d(\hat{C}_{j,k}^{(l_j)})$ represents the highpass downsampling result achieved by quadrature mirror filter; β is the parameter defined by different thresholds. For soft thresholding, the value of β is 0.33. For hard thresholding, we choose 3 as β.

(5) After thresholding, we obtain $\tilde{C}_{j,k}^{(l_j)}$. Then, an inverse contourlet transform is implemented to obtain recovered image z.

(6) Finally, z is applied an adaptive wiener method based on statistics [16] to denoise and obtain reconstruction x_{rec}.

We use the neighborhood of each pixel to estimate the local mean written as μ and local variance denoted as σ^2.

$$\mu = \frac{1}{16}\sum_{a,\,b\in\eta} z(a,b) \quad \sigma^2 = \frac{1}{16}\sum_{a,\,b\in\eta} Z^2(a,b) - \mu^2$$

where η is a 4×4 neighborhood around each pixel of image z

$$x_{rec}(a,b) = \mu + \frac{\sigma^2 - \overline{\sigma^2}}{\sigma^2}(z(a,b)-\mu)$$

where $\overline{\sigma^2}$ is the average of all local estimated variances.

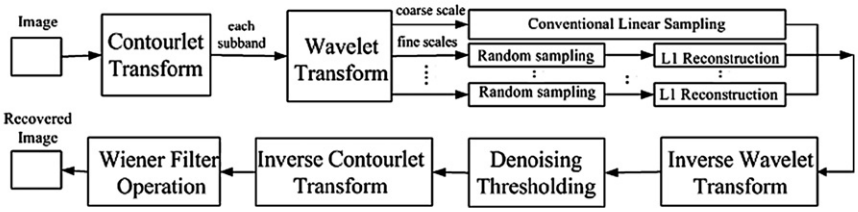

Fig. 4. The flowchart of CS reconstruction based on wavelet in the contourlet domain.

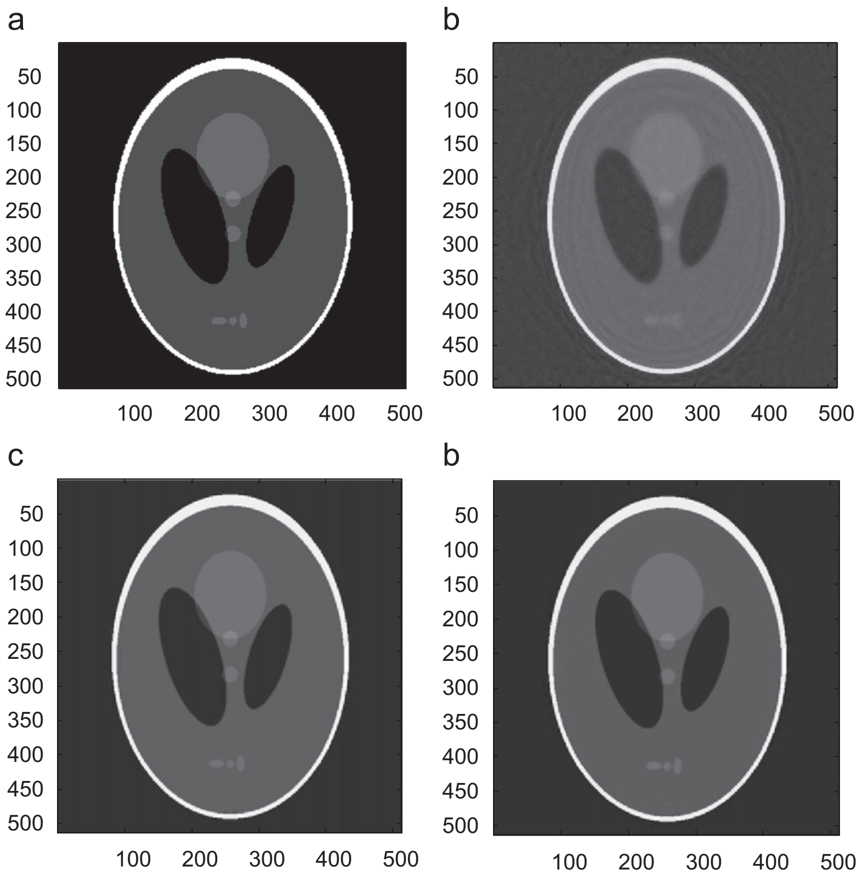

Fig. 5. Recovered image 'Sheep-Logan Phantom': (a) original image 'Shepp-Logan Phantom' $\|x-x\|_2=0$, (b) reconstruction from CS based on the curvelet frame [2] by BP, SM=22,528 × 90,112, $\|x_{curvelet}-x\|_2=0.134$, (c) reconstruction from CS based on wavelet transform in the contourlet domain by BP, S_{max}=1843 × 3072, $\|x_{contourlet}-x\|_2=0.1298$, and (d) reconstruction from CS based on wavelet transform in the contourlet domain by BCS, S_{max}=1843 × 3072, $\|x_{contourlet}-x\|_2=0.1283$.

The flowchart of the proposed method is listed in Fig. 4.

From the above flowchart, we can see (i) each directional contourlet subband is transformed by wavelet, and then we apply multiscale compressed sensing on each one; (ii) the coarse and fine scales (random sampling scales) of wavelet in each subband are chosen automatically. They may be different at different subbands, which imply different sizes of random matrices.

4. Simulation

First, in order to make comparison with CS based on curvelet [2], we start with a 512×512 medical image 'Sheep-Logan Phantom'. Fig. 5(a) shows the original image, and the reconstruction from CS based on curvelet transform is shown in Figs. 5(b), (c) and (d) are recovered images from CS based on the wavelet transform in the contourlet domain. Meanwhile, Fig. 5(c) uses BP and Fig. 5(d) applies BCS. S_M denotes the size of random measurement matrix. $S_{\max}$ represents the maximum size of random measurement matrices by using the proposed method.

From the above simulation, the quality of reconstruction based on the proposed algorithm is better than that on curvelet in criteria of l_2 norm error. In fact, contourlet and curvelet transforms both fall into the field of multiscale geometric analysis (MGA), but the former offers more sparse representations for discrete signals. So the CS recovered result by the proposed method is better. We should also notice that the size of random matrix is $22{,}528 \times 90{,}112$ in Fig. 5(b) and the maximum size among the random matrices is 1843×3072, as shown in Fig. 5(c) and (d). It is clear that the computation and the storage of random measurement matrices reduce since we do not necessarily generate large size matrix in the CS reconstruction. In fact, this paper introduces the wavelet transform into the contourlet domain. Only the gathered nonzero coefficients are measured in CS, thus the size of the random measurement matrix in our algorithm is much smaller than that size we get from CS based on curvelets [2]. This leads to another question: why we introduce wavelet transform into the contourlet domain rather than introduce it into the spatial domain?

So another two standard images—'Lena' and 'Peppers' are recovered by CS based on wavelet and by the proposed method, as shown in Figs. 6 and 7.

For fair comparison, we use the same sizes of random matrices in each contourlet subband, which implies the

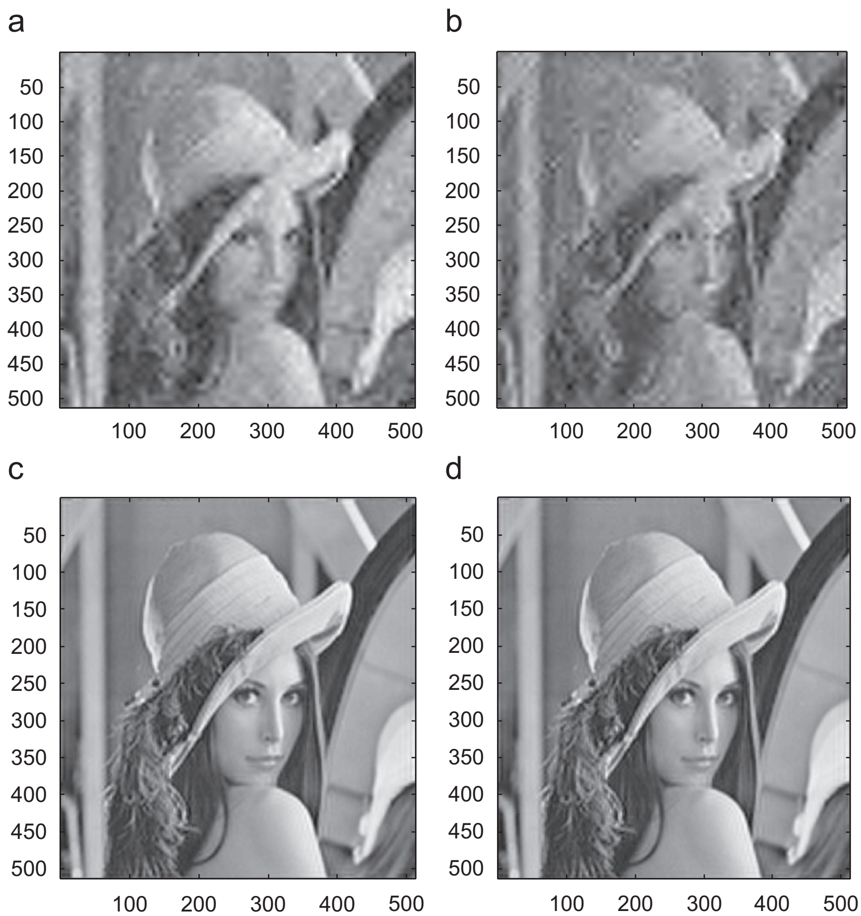

Fig. 6. Recovery results of image 'Lena': (a) reconstruction from CS based on wavelet [2] by BP, $S_{\max}=1536 \times 3072$, PSNR=29.437, (b) reconstruction from CS based on wavelet [2] by BCS, $S_{\max}=1536 \times 3072$, PSNR=28.069, (c) reconstruction from CS based on the proposed method by BP, $S_{\max}=1536 \times 3072$, PSNR=36.194, and (d) reconstruction from CS based on the proposed method by BCS, $S_{\max}=1536 \times 3072$, PSNR=36.181.

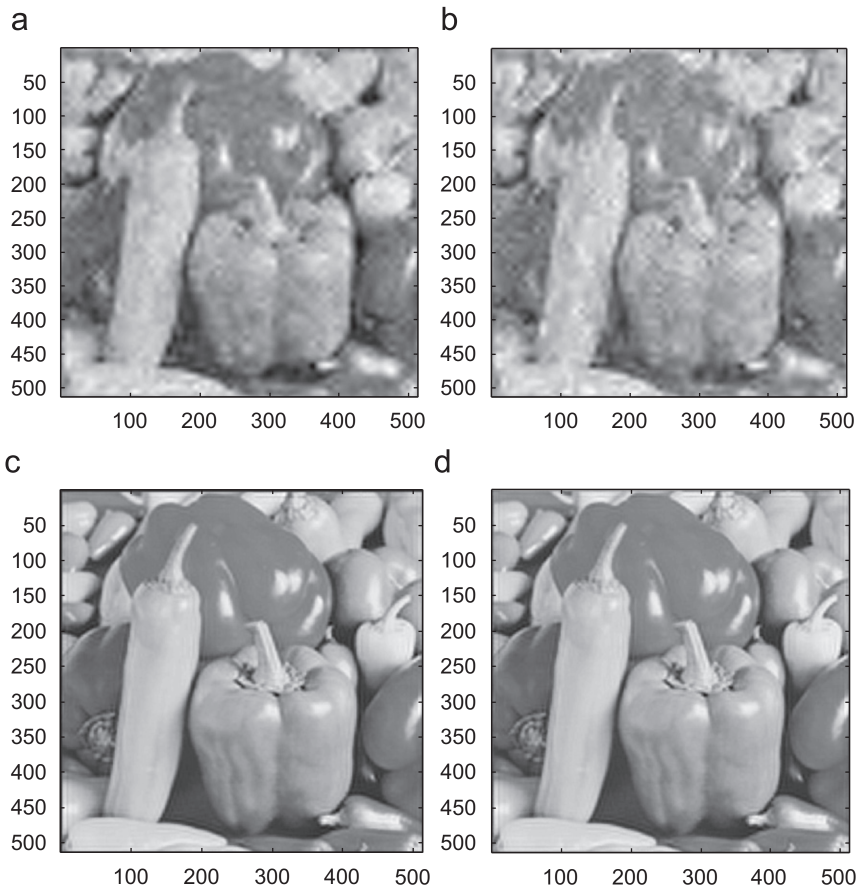

Fig. 7. Recovery results of image 'peppers': (a) CS recovered result based on wavelet [2] using BP, $S_{\max}$=1843 × 3072, PSNR=28.82, (b) CS recovered result based on wavelet [2] using BCS, $S_{\max}$=1843 × 3072, PSNR=27.294, (c) CS recovered result based on the proposed method using BP, $S_{\max}$=1843 × 3072, PSNR=35.901, and (d) CS recovered result based on the proposed method using BCS, $S_{\max}$=1843 × 3072, PSNR=35.895.

same coarse and fine scales are used among the simulations below, and then adopt BP and BCS optimization methods, respectively. The CS recovered images based on the proposed method and on the wavelet [2] are both listed in Figs. 6 and 7. The above two methods use the same way to choose the sampling matrices (see Eq. (3)). The quality of recovered images is measured by the peak signal to noise ratio (PSNR between the original image x and the recovered image $x_{\text{contourlet}}$), $PSNR(x, x_{contourlet}) = 20\log 10(\|x - x_{contourlet}\|_2/512)$. In these two experiments, the coarse scale is 4, and the fine scales are 5 and 6. $S_{\max}$ denotes the maximum size of the random sampling matrix.

Under the condition of the same sizes of random measurement matrices and the same optimal methods, the reconstruction quality by the proposed algorithm is improved through the PSNR comparison. As only the wavelet transform is used in the CS reconstruction, the computational burden of CS based on wavelets [2] is comparably small; however, wavelets could not provide the sparsest representation. So the quality of reconstruction is not ideal. That is why the algorithm of the compressed sensing based on the wavelet transform in the contourlet domain is proposed.

From the above experiments, when we use the method of CS based on wavelets [2], the quality of reconstruction should be further improved. Meanwhile, when the method of CS based on curvelets [2] is used, the size of measurement matrix required in random sampling is so large that it makes the computation and the storage of the matrix too difficult. The sizes of measurement matrices are small with high reconstruction quality, when we use the proposed method.

This paper makes full use of sparse representation ability of the contourlet frame, which is required in the CS reconstruction, and introduces the wavelet transform into contourlet domain so as to reduce the computation and the storage of random measurement matrices. So the proposed algorithm image compressed sensing based on the wavelet transform in the contourlet domain is feasible and of higher reconstruction quality.

5. Conclusion

In this paper, we successfully implement a CS recovered system based on wavelet transform in the contourlet domain. Due to the sparse representation ability of contourlet basis and wavelet transform, which decreases the size of random measurement matrix, images are recovered with higher quality and lower computation and storage. Meanwhile, there are some works that call for further consideration. Firstly, decomposition scale in contourlet domain and reconstruction performance should be balanced in the future. Secondly, the application of this method into the noisy image will be considered. Finally, the CS framework based on contourlets should be extended and other methods to reduce the size of random matrix will be studied.

Acknowledgements

The authors want to express appreciation to Mr. Z.K. Yin and his researcher team for sharing and discussing some problem. They would also like to say thanks to Ms. Y. Huang for clarifying on English usage.

References

[1] E.J. Candes, J. Romberg, Practical signal recovery from random projections, in: Proceedings of the SPIE 5914 (2005).
[2] Y. Tsaig, D.L. Donoho, Extensions of compressed sensing, Signal Processing 86 (3) (2006) 533–548.
[3] D.L. Donoho, M.R. Duncan, Digital curvelet transform: strategy, implementation and experiments, in: Proceedings of the SPIE 4056 (2000) 12–29.
[4] R. G. Baraniuk, V. Cevher Model-based compressive sensing (2008). Available at 〈http://people.ee.duke.edu/~lcarin/baraniuk.pdf〉.
[5] S SChen, D.L. Donoho, A. Saunders, Atomic decomposition by basis pursuit, SIAM Review 43 (1) (2001) 129–159.
[6] S. Ji, Y. Xue, L. Carin, Bayesian compressive sensing, IEEE Transactions on Signal Process 56 (6) (2008) 2346–2356.
[7] D.L. Donoho, Y. Tsaig, I. Drori, J-C. Starck, Sparse solution of underdetermined linear equations by stagewise orthogonal matching pursuit, Technical Report (Department of Statistics, Stanford University): March (2006). 〈http://stat.stanford.edu/~idrori/StOMP.pdf〉.
[8] D.L. Donoho, Compressed sensing, IEEE Transactions on Information Theory 52 (4) (2006) 1289–1306.
[9] E.J. Candes, M.B. Wakin, An introduction to compressive sampling, IEEE Signal Processing Magazine 25 (2) (2008) 21–30.
[10] Minh N. Do, Martin Vetterli, Contourlets, in Beyond Wavelets, J.Stoeckler and G.V.Welland, Eds. Academic Press, New York, (2003), to appear, 〈http://www.ifp.uiuc.edu/~minhdo/publications〉.
[11] Minh N. Do, Vetterli Martin, The contourlet transform: an efficient directional multiresolution image representation, IEEE Transactions on Image Processing 52 (4) (2006) 1–15.
[12] P.J. Burt, E.H. Adelson, The Laplacian pyramid as a compact image code, IEEE Transactions on Communication 31 (4) (1983) 532–540.
[13] R.H. Bamberger, M.J.T. Smith, A filter bank for the directional decomposition of images: the theory and design, IEEE Transactions on Signal Processing 40 (4) (1992) 882–893.
[14] J.L. Chen, Development and prospect of image multiscale geometric analysis, Acta Electronica Sinica 31 (12) (2003) 1975–1980.
[15] Qiu S.L., Image compressed sensing based on DT-CWT, ICALIP2008.
[16] Jae S. Lim, Two-Dimensional Signal and Image Processing, Prentice Hall, Englewood Cliffs, NJ, 1990, 536–540.